A Flag structure on a cusped hyperbolic 3-manifold with unipotent holonomy.

Elisha Falbel, Rafael Santos Thebaldi

HAL Id: hal-00958255

https://hal.archives-ouvertes.fr/hal-00958255

Submitted on 14 Mar 2014

A FLAG STRUCTURE ON A CUSPED HYPERBOLIC 3-MANIFOLD WITH UNIPOTENT BOUNDARY HOLONOMY

ELISHA FALBEL AND RAFAEL SANTOS THEBALDI

ABSTRACT. A Flag structure on a 3-manifold is an (X, G) structure where $G = \mathrm{SL}(3, \mathbb{R})$ and X is the space of flags on the 2-dimensional projective space. We construct a flag structure on a cusped hyperbolic manifold with unipotent boundary holonomy. The holonomy representation can be obtained from a punctured torus group representation into $\mathrm{SL}(3, \mathbb{R})$ which is equivariant under a pseudo-Anosov.

1. INTRODUCTION

A Flag structure on a 3-manifold is an (X, G) structure where $G = \mathrm{SL}(3, \mathbb{R})$ and X is the space of flags on the 2-dimensional projective space. That is the space of pairs: point and line containing it. The most direct construction of such structures starts with a real projective surface or orbifold. The projectivization of its tangent bundle is a Seifert manifold and has a natural flag structure. Other constructions on Seifert manifolds are studied in [1]. Note that projective structures on 3-manifolds concern instead the group $\mathrm{SL}(4, \mathbb{R})$ (see [3]).

Representations of fundamental groups of three manifolds into $\mathrm{SL}(3, \mathbb{R})$ were obtained in [6] following the method described in [2]. A fundamental question is whether these representations correspond to holonomies of flag structures on the manifold.

The goal of this paper is to construct a flag structure on a cusped hyperbolic manifold with unipotent boundary holonomy (see Theorem 6.8). We introduce a general method of construction via gluings of tetrahedra which are defined on the flag space. The tetrahedra are canonical up to a finite choice related to an order on the 0-skeleton of an ideal triangulation of the manifold once one fixes a decoration (that is a choice of a flag at each vertex) satisfying certain compatibility conditions (see [2]). Definitions of simplices in Grassmanian spaces (although not containing the case of flag space) were also considered in [7] and inspired us for our definition of tetrahedron.

The method presented here can be considered as a flag structure analog of Thurston's construction of hyperbolic structures on cusped manifolds by gluing ideal hyperbolic tetrahedra ([8]) and of the construction of CR structures as in [5].

The holonomy representation of the structure we obtained is not faithful. It turns out that the manifold $m009$ we analyzed here has holonomy group contained in a triangle group of type $(3, 3, 5)$ (see the end of the appendix). An isomorphic triangle group was obtained in [4] where the holonomy representation has values in $\mathrm{PU}(2, 1)$. These representations are Galois conjugates as explained in [6], indeed, they are all parametrized by solutions of a degree four irreducible polynomial in

1

one variable. Two solutions correspond to conjugate representations in $\mathrm{PU}(2,1)$ and the other two to two dual flag structures.

It is interesting to remark that the manifold m009 is fibered over the circle with fiber a punctured torus. The representation into $\mathrm{SL}(3, \mathbb{R})$ of the fiber surface group is then equivariant with respect to the mapping class group element defining the bundle.

2. Flag structures on 3-manifolds

A Flag structure on a 3-manifold is an (X, G) structure where X is a homogeneous space described in the following paragraph and $G = \mathrm{SL}(3, \mathbb{R}) = \mathrm{PGL}(3, \mathbb{R})$.

The homogeneous space X is the space of flags in $\mathbb{P}(\mathbb{R}^3)$. An affine flag in $V = \mathbb{R}^3$ is a couple (line, plane), the line belonging to the plane. They project to flags in $\mathbb{P}(V)$, that is, couples (point, line). Using the dual vector space V^* and the projective spaces $\mathbb{P}(V)$ and $\mathbb{P}(V^*)$, define the spaces of *flags* $\mathcal{F}l$ by the following:

$$\mathcal{F}l \quad = \quad \{([x], [f]) \in \mathbb{P}(V) \times \mathbb{P}(V^*) \,|\, f(x) = 0\}.$$

The action of $\mathrm{SL}(3, \mathbb{R})$ on V induces an action on $\mathbb{P}(V) \times \mathbb{P}(V^*)$. Indeed, identify V and V^* using the canonical scalar product and then, via this identification, the contragredient action (that is $g.v = (g^{-1})^T v$) on V^*. We note π_1 and π_2 the two projections of $\mathcal{F}l$ into $\mathbb{P}(V)$ and $\mathbb{P}(V^*)$ respectively.

Observe that

$$\mathcal{F}l = \mathrm{SL}(3, \mathbb{R})/B,$$

where B is the Borel subgroup of upper-triangular matrices in $\mathrm{SL}(3, \mathbb{R})$. The flag space is identified to the projectivization of the tangent bundle to $P(V)$ and the differential action of $\mathrm{SL}(3, \mathbb{R})$ on the tangent bundle induces the above action. Observe that, in fact, $\mathrm{SL}(3, \mathbb{R})$ acts on the unit tangent bundle of $P(V)$ (which has S^3 as a double cover) and therefore the double cover of $\mathrm{SL}(3, \mathbb{R})$ (which is simply connected) acts on the sphere S^3.

2.1. **Definition.** A flag structure on a 3-manifold M is a $(\mathcal{F}l, \mathrm{SL}(3, \mathbb{R}))$ structure on that manifold.

The involution $\Theta(v, w) = (w, v)$ defined on $\mathcal{F}l$ and the Cartan involution $\theta(g) = (g^{-1})^T$ defined on $\mathrm{SL}(3, \mathbb{R})$ satisfy

$$\Theta \circ g = \theta(g) \circ \Theta.$$

Given a flag structure on a 3-manifold, we call dual flag structure the structure obtained by using transition functions composed with θ.

2.2. **Coordinates in $\mathbb{P}(V)$.** To make possible a visualization of the flags we will choose a chart (called *prefered chart*) on $\mathbb{P}(V)$. Consider the hyperplane in $\mathbb{R}^3$ defined by the three basis unit vectors, that is

$$x + y + z = 1.$$

The chart is defined by projecting lines passing through the origin in that hyperplane and imposing that

$$[1, 0, 0] \to (0, 0), \quad [0, 1, 0] \to (1, 0), \quad [0, 0, 1] \to (0, 1).$$

Observe than that, on the hyperplane,

$$[x, y, z] \to (y, z).$$

In particular $[1, 1, 1] \to (\frac{1}{3}, \frac{1}{3})$.

Given a flag $[[x, y, z], [a, b, c]]$, with $x + y + z = 1$, the line on $\mathbb{P}(V)$ defined by the image of the plane orthogonal to the vector (a, b, c) is described in the chart above by:

- the point (y, z),
- the line defined by the vector $(a - c, b - a)$ passing through the point (y, z).

Therefore the line makes an angle θ satisfying $\tan \theta = \frac{b-a}{a-c}$ with the horizontal direction. Figure 1 shows, three flags corresponding to planes passing through the three basis vectors in $\mathbb{R}^3$.
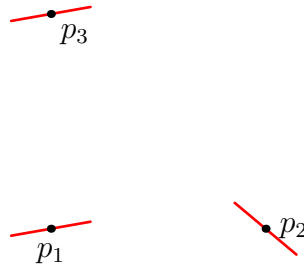

FIGURE 1. Three flags corresponding to planes passing through the three basis vectors in $\mathbb{R}^3$

3. EDGES

One can join a couple of flags by simple paths (see Figure 2) but there is a canonical construction of a unique line containing two flags.
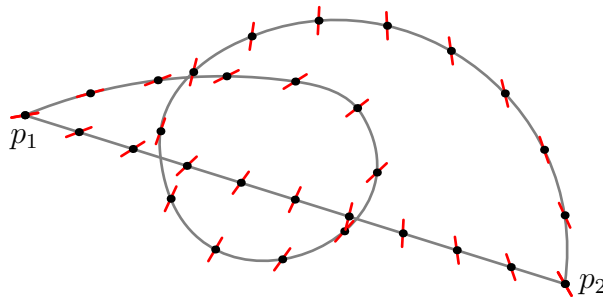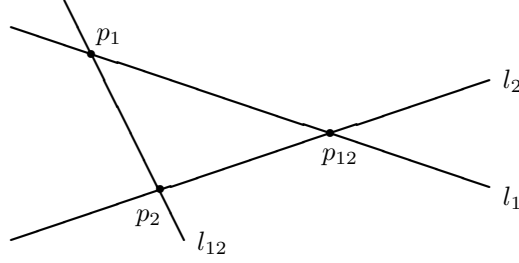

FIGURE 2. Two simple paths of flags projected into $\mathbb{P}(V)$.

Consider two flags in generic position, that is, $f_1 = (p_1, l_1)$, $f_2 = (p_2, l_2)$ such that $l_i(p_j) \neq 0$ if $i \neq j$.

FIGURE 3. Points and lines fixed by H_{12}^0.

The action of $\mathrm{SL}(3, \mathbb{R})$ is transitive on these pairs. There exists a unique point p_{12} such that $l_i(p_{12}) = 0$, for $i = 1, 2$. Up to the action of $\mathrm{SL}(3, \mathbb{R})$ we can normalize so that

- $p_1 = (1, 0, 0)$, $l_1 = (0, 1, 0)$,
- $p_2 = (0, 1, 0)$, $l_2 = (1, 0, 0)$

The intersection point of the two lines is $p_{12} = (0, 0, 1)$. Projective transformations fixing the three points are diagonal and they preserve the line $[p_1, p_2]$. For each line l passing through p_{12} we consider its intersection p with the line $[p_1, p_2]$ (see Figure 4). This defines a circle of flags (p, l) containing f_1 and f_2. It is divided in two segments with boundaries the two given flags. Following [7] we let H_{12}^0 be the connected component of the identity of the group preserving the points p_1, p_2, p_{12}. It preserves the lines l_1, l_2, l_{12} (see Figure 3) and the two segments are orbits of its action on the space of flags whose closure contains the flags f_1 and f_2. In the normalization above we have

$$H_{12}^0 = \begin{bmatrix} h_1 & 0 & 0 \\ 0 & h_2 & 0 \\ 0 & 0 & h_3 \end{bmatrix}$$

with $h_i > 0$. The circle of flags is given by

$$p = [\lambda_1, \lambda_2, 0], \quad l = [\lambda_2, -\lambda_1, 0].$$

More generally, if $f_1 = (p_1, l_1)$, $f_2 = (p_2, l_2)$ are two flags in generic position than the line containing the flags is

$$\left(\lambda_1 p_1 + \lambda_2 p_2, \frac{\lambda_2}{l_2(p_1)} l_2 - \frac{\lambda_1}{l_1(p_2)} l_1 \right).$$

The line is divided in two segments corresponding to the relative signs of λ_1 and λ_2.

A simple property of a segment between two flags is stated in the following lemma. It is the basic technical resut we need to construct the tetrahedra of flags and will be repeatedly used in the analysis of the example in the last section.

3.1. **Lemma** (monotonicity Lemma). *Let $f_1 = (p_1, l_1)$, $f_2 = (p_2, l_2)$ be two flags. Suppose, in the preferred chart, the angles of the projected lines are $0 \leq \theta_1 \leq \theta_2 \leq \pi$. Then, along the finite segment from f_1 to f_2, the angles of the projected lines are increasing (and satisfy $\theta_1 \leq \theta \leq \theta_2$).*
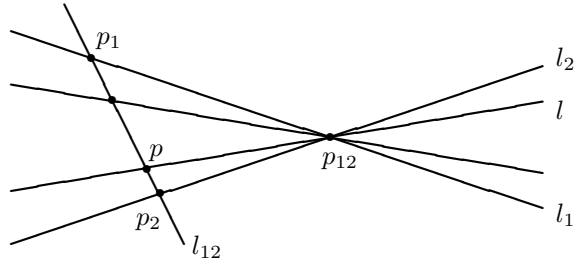
FIGURE 4. A segment between two flags.

Moreover, if $f_2' = (p_2, l_2')$ is another flag such that $\theta_2 \leq \theta_2'$ then, along the corresponding segment, the angles of the projected lines satisfy $\theta \leq \theta'$.
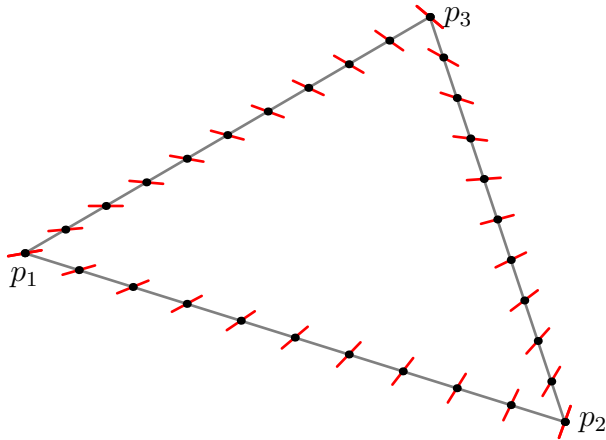
4. TRIANGLES

FIGURE 5. A triangle of flags projected into $\mathbb{P}(V)$.

By a *generic configuration of flags* $([x_i], [f_i])$, $1 \leq i \leq n+1$ we understand $n+1$ points $[x_i]$ in general position and $n+1$ lines l_i in $\mathbb{P}(V)$ such that $l_j(x_i) \neq 0$ if $i \neq j$. Recall that a configuration of ordered points in $\mathbb{P}(V)$ is said to be in *general position* when no three points are contained in the same line. Remark that we give priority to the points in the above definition and don't impose that the lines are in generic position.

Let e_1, e_2, e_3 be the canonical basis of V and (e_1^*, e_2^*, e_3^*) its dual basis. Up to the action of $\mathrm{SL}(3, \mathbb{R})$, a generic configuration of three flags $([x_i], [l_i])_{1 \leq i \leq 3}$ can be normalized, in these coordinates, as

- $x_1 = (1, 0, 0)$, $l_1 = (0, 1, 1)$,
- $x_2 = (0, 1, 0)$, $l_2 = (1, 0, 1)$ and
- $x_3 = (0, 0, 1)$, $l_3 = (z, 1, 0)$ with $z \neq 0$.

Therefore the only invariant of a generic configuration of three flags (up to $\mathrm{SL}(3,\mathbb{R})$) is given by the triple ratio

$$z = \frac{l_1(x_2)l_2(x_3)l_3(x_1)}{l_1(x_3)l_2(x_1)l_3(x_2)} \in \mathbb{R}^\times$$

Remark that the three lines of the triple of flags are linearly independent if and only if $z \neq -1$.

Given three flags in general position $f_1 = (p_1, l_1), f_2 = (p_2, l_2), f_3 = (p_3, l_3)$ we may form a triangle (a 1-skeleton as in Figure 5) containing them by choosing three edges as above. There are 8 possible choices, namely for each couple of flags in a chart one can choose either the bounded segment or the unbounded segment with end points given by the two flags.

Fixing a choice of edges we define a *face* as an embedded 2-simplex whose boundary is the union of the three edges. Observe that this imposes a restriction on the 1-simplex; it should be null-homotopic. In particular, the projections by π_1 and π_2 of the 1-skeleton should be null-homotopic. If the edges are as in the previous section there is a restriction on the triple-ratio of a triple of flags:

4.1. Lemma. *A triple of flags defines a null-homotopic canonical 1-skeleton if and only if the triple ratio of the three flags is negative. In that case there are precisely four canonical 1-skeletons which are null homotopic.*

The proof of the lemma consists of comparing the two possible situations which give negative and positive triratios in the following Figures 6 and 7. To obtain the sign of the triratio one simply counts the number of times the lines separate the points not contained in them.

Once the 1-skeleton is defined we should define a 2-simplex whose boundary is the given 1-skeleton. A particular canonical choice is given as a union of segments:

4.2. Definition. A face F_{123} in the flag space with vertices f_i, $i = 1, 2, 3$ (with negative triple ratio) and a choice of edges $[f_1, f_2], [f_2, f_3], [f_3, f_1]$ is the 2-skeleton which is the union of segments between f_1 and f_t where $f_t \in [f_2, f_3]$, that is,

$$F_{123} = \{f \in \mathcal{F}l \mid f \in [f_1, f_t] \text{ for } f_t \in [f_2, f_3] \}.$$

The flag f_1 is called the *source of the face* . Remark that given a triple of flags with negative triple ratio, the surface obtained is embedded with boundary the union of edges only for two choices of the source.

If the triple of flags has positive triple ratio it will be impossible to fill up a triangle unless we change the 1-skeleton in the following way: in the configuration represented in the figure below there is a flag $f_0 = (p_0, l_0) \in [f_2, f_3]$ such that $p_1 \in l_0$ so that the flags f_0 and f_1 are not in general position. In order to define the triangle we should add, along the points $p \in [p_0, p_1]$ the flags (p, l_0) and over the point p_1 the flags $\pi_1^{-1}(p_1)$. In this way the projection of the 1-skeleton is twice the generator and therefore it is null-homotopic. In this paper, though, we will only use triples with negative ratio.

The 1-skeleton determines a triangle $T_{123} \subset \mathbb{P}(V)$ when projected by π_1 and $T_{123}^* \subset \mathbb{P}(V^*)$ when projected by π_2. The following straightforward Lemma helps computing intersections between faces.

4.3. Lemma.
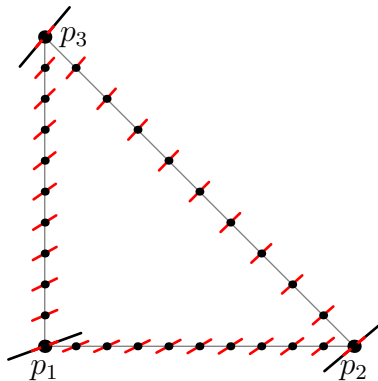$$\pi_1(F_{123}) = T_{123}, \quad \pi_2(F_{123}) = T_{123}^*.$$

FIGURE 6. Three flags and segments joining them projected in the preferred chart. We only draw the finite triangle. The Euler number of a vector field parallel to the line field along the triangle is 0. The triratio is negative.
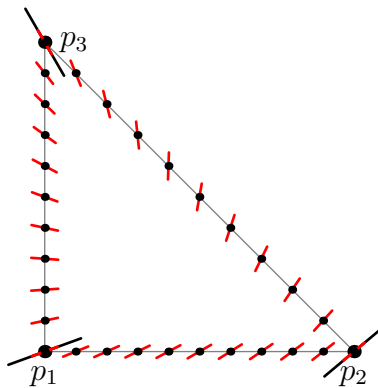

FIGURE 7. Three flags and segments joining them projected in the preferred chart. The Euler number of a vector field parallel to the line field is of absolute value 1. The triratio is positive.

5. COORDINATES ON A FLAG TETRAHEDRON

In this section we recall the coordinates parametrizing configurations of four flags in the projective space $\mathbb{P}(\mathbb{R}^3)$ as in [2, 6].

5.1. **Coordinates for a tetrahedron of flags.** Let $([x_i], [f_i])_{1 \leq i \leq 4}$ be a generic tetrahedron. Dispose symbolically these flags on a tetrahedron 1234 as in Figure 9. We define a set of 12 coordinates on the edges of the tetrahedron (1 for each oriented edge).

To define the coordinate z_{ij} associated to the edge ij, we first define k and l such that the permutation $(1, 2, 3, 4) \mapsto (i, j, k, l)$ is even. The pencil of (projective) lines through the point x_i is a projective line $\mathbb{P}_1(k)$. We have four points in this projective line: the line $\ker(f_i)$ and the three lines through x_i and one of the x_l for $l \neq i$. We define z_{ij} as the cross-ratio of four flags by

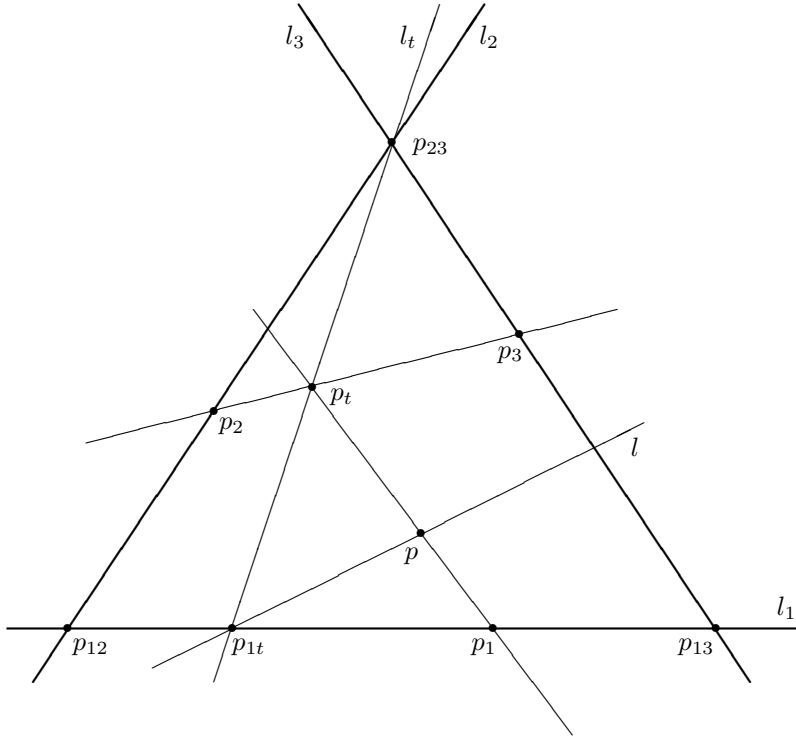$$z_{ij} := [\ker(f_i), (x_i x_j), (x_i x_k), (x_i x_l)].$$

FIGURE 8. A synthetic construction of the flag (p, l) in the face F_{123}.

Note that we follow the usual convention that the cross-ratio of four points x_1, x_2, x_3, x_4 on a line is the value at x_4 of a projective coordinate taking value ∞ at x_1, 0 at x_2, and 1 at x_3. Figure 9 displays the coordinates.

At each face (ijk) (oriented as the boundary of the tetrahedron (1234)), we associate the 3-ratio:

$$z_{ijk} = \frac{f_i(x_j)f_j(x_k)f_k(x_i)}{f_i(x_k)f_j(x_i)f_k(x_j)}.$$

Observe that if the same face (ikj) (with opposite orientation) is common to a second tetrahedron then

$$z_{ikj} = \frac{1}{z_{ijk}}.$$

Of course there are relations between the whole set of coordinates. Fix an even permutation (i, j, k, l) of $(1, 2, 3, 4)$. First, for each face (ijk), the 3-ratio is the opposite of the product of all cross-ratios "leaving" this face:

(5.1.1) $z_{ijk} = -z_{il}z_{jl}z_{kl}.$
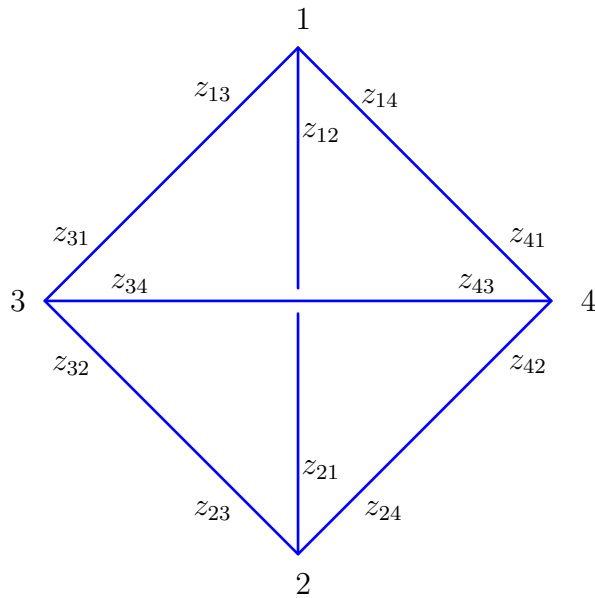
FIGURE 9. The z-coordinates.

Second, the three cross-ratio leaving a vertex are algebraically related:

$$z_{ik} = \frac{1}{1 - z_{ij}}$$

(5.1.2)

$$z_{il} = 1 - \frac{1}{z_{ij}}$$

The next proposition shows that a tetrahedron is uniquely determined, up to the action of $\mathrm{SL}(3, \mathbb{R})$, by four numbers.

5.2. **Proposition.** *The space of generic tetrahedra is parametrized by the 4-tuple* $(z_{12}, z_{21}, z_{34}, z_{43})$ *of elements in* $\mathbb{R} \setminus \{0, 1\}$.

In particular, one can normalize the coordinates of four flags up to the action of $\mathrm{SL}(3, \mathbb{R})$ as follows

(1) f_1: $x_1 = (1, 0, 0)$, $l_1 = (0, z_{14}, -1)$,
(2) f_2: $x_2 = (0, 1, 0)$, $l_2 = (1/z_{24}, 0, -1)$,
(3) f_3: $x_3 = (0, 0, 1)$, $l_3 = (z_{34}, -1, 0)$,
(4) f_4: $x_4 = (1, 1, 1)$, $l_4 = (z_{42}, 1/z_{41}, -1)$.

6. EXAMPLE: m009

The manifold m009 is an open manifold which has a complete hyperbolic structure with finite volume. It is obtained by gluing three tetrahedra $T_0(u_i), T_1(v_i)$ and $T_2(w_i)$ as shown in Figure 10.

The face identifications are the following: $(234)^0 \leftrightarrow (243)^1$, $(142)^0 \leftrightarrow (314)^1$, $(134)^0 \leftrightarrow (143)^2$, $(123)^0 \leftrightarrow (213)^2$, $(142)^1 \leftrightarrow (241)^2$ and $(123)^1 \leftrightarrow (342)^2$.

In [6] we obtained a particular realization of these tetrahedra by 4-tuples of flags giving rise to representations into $\mathrm{SL}(3, \mathbb{R})$ with unipotent boundary holonomy. The
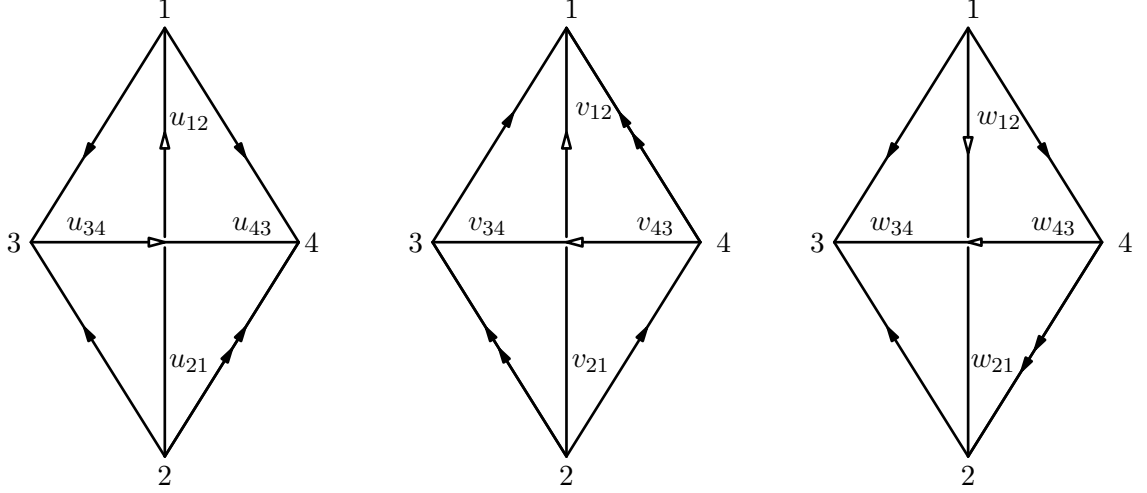
FIGURE 10. Three tetrahedra glued to obtain the manifold m009. The tetrahedra are numbered from 0 to 2 from left to right.

invariants of the 4-tuple of flags all depend on $\gamma = -\frac{1}{2} + \frac{1}{2}\sqrt{5 + 4\sqrt{5}}$. Explicitly:

$$u_{12} = w_{34} = \frac{\gamma+3}{\gamma+1},\ u_{21} = w_{43} = \gamma,\ u_{34} = w_{12} = \frac{\gamma-2}{\gamma},$$
$$u_{43} = w_{21} = -1 - \gamma,\ v_{12} = v_{34} = \frac{1}{\gamma+3},\ v_{21} = v_{43} = \frac{1}{2-\gamma}.$$

The group obtained has rank one boundary holonomy and one can chose generators called meridian g_M and longitude g_L satisfying $g_M g_L^2 = 1$.

The realization described above comes in pair with another one giving rise to a dual flag structure. It is also related to a representation of the fundamental group in $PU(2,1)$ with boundary holonomy of rank one which seems to give rise to a uniformizable CR structure on m009 ([4]).

6.1. **The tetrahedron T_0.** Using the coordinates above, the four flags $f_i = [p_i, l_i]$, $1 \leq i \leq 4$, defining T_0 can be represented in the preferred chart as in Figure 11. We choose the segments between the flags so that all of them are finite and contained in the preferred chart.

The remaining part of this subsection contains the proof of the following proposition.

6.2. **Proposition.** *The four flags defining T_0 and the 1-skeleton E_{ij} (defined by the finite segments joining the flags i and j in the preferred chart) can be extended to a simplex with faces F_{314}^0, F_{342}^0, F_{412}^0, F_{312}^0.*

We need to construct the four faces of the tetrahedron and verify that their intersections are precisely their common edges. They are (where we write, to simply notations, $F_{ijk}^0 = F_{ijk}$):

$$F_{314},\ F_{342},\ F_{412},\ F_{312}.$$

Clearly, the first three faces only intersect in their common edges. The only verification to be done is on the intersection of these faces with F_{312}. We need to prove:
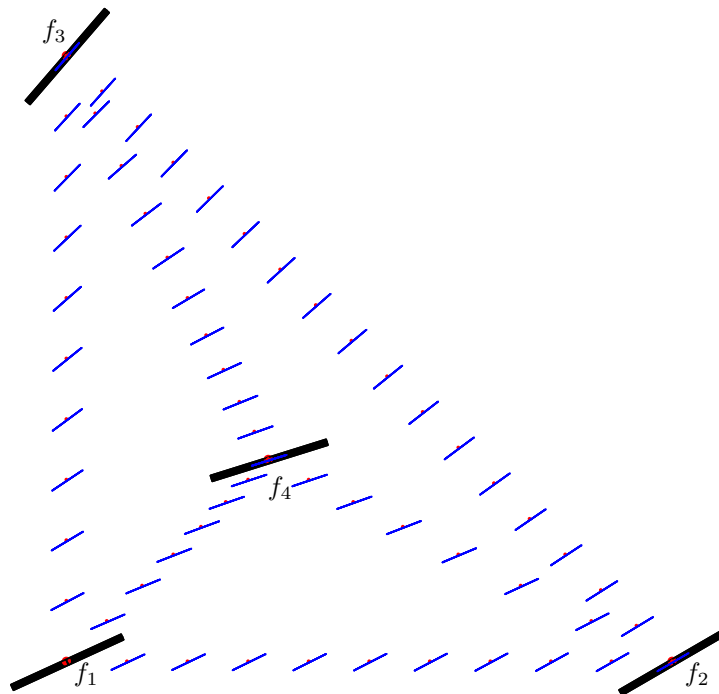
(1) $F_{412} \cap F_{312} = E_{12}$,

FIGURE 11. The four flags of tetrahedron T_0 and segments joining them projected in the preferred chart. Here $\theta_4 < \theta_1 < \theta_2 < \theta_3$.

(2) $F_{314} \cap F_{312} = E_{31}$,
(3) $F_{342} \cap F_{312} = E_{32}$.

The argument uses Lemma 3.1 in a simple way. We choose the preferred chart. Observe first, because $\theta_4 < \theta_1 < \theta_2$, that the segment E_{12} has all flags with angles greater than the flags at the edges E_{14}. By the Lemma we have then that $F_{314} \cap F_{312} = E_{31}$.

Observe that the line from p_3 to p_4 intersects the edge E_{12} at a point, say p, whose flag has angle $\theta > \theta_4$. Moreover a simple drawing (see Figure 6.1) or computation shows that the intersection point of l_4 with the line l_2 is between p_2 and the intersection point between l_1 and l_2. This is sufficient to prove that the angle of a flag along the segment E_{24} is smaller than the corresponding flag (along the segment whose projection contains p_3 and the projection of the flag in E_{24}) passing at the edge E_{12}.

This implies, again by the Lemma, that $F_{342} \cap F_{312} = E_{32}$.

To analyse $F_{412} \cap F_{312}$, observe that if x belongs to the triangle $p_1 p_2 p_4$ and is to the left of the line $p_3 p_4$ then, because $\theta_1 < \theta_2$ we obtain that the angle at x along the line from p_3 is greater than the angle along the line from p_4. For a point to the right of the line $p_3 p_4$, we conclude with an argument analogous to the previous paragraph. This implies again that $F_{412} \cap F_{312} = E_{12}$.
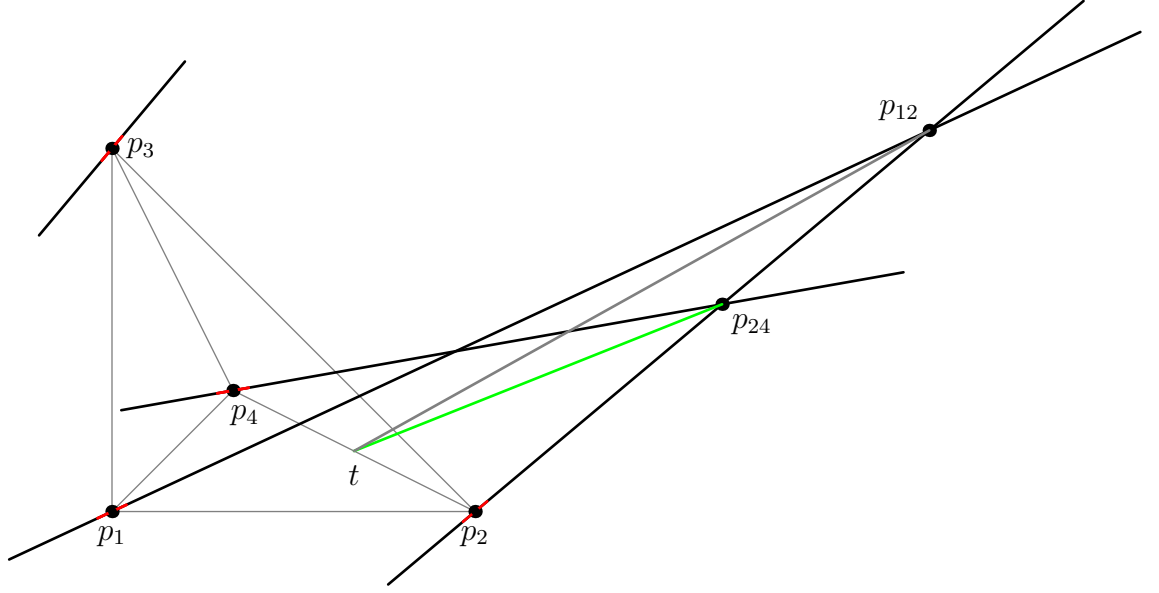
FIGURE 12. Comparison of two flags over a point $t \in p_2p_4$. At the point t the flag of the face F_{312} has greater angle than the one of the face F_{342}.

6.3. **The other two tetrahedra T_1 and T_2.** In Figure 13 we show the three tetrahedra glued according to $g_1 : (243)^1 \to (234)^0$ and $g_2 : (142)^2 \to (241)^1$. The points in the Figure are projections of the following flags: $f_5 = [p_5, l_5] = g_1[p_1, l_1]$ and $f_6 = [p_6, l_6] = g_1g_2[p_3, l_3]$.

Due to the face pairings, the faces of T_1 and T_2 are in part determined by the choice of the faces of T_0. Namely, for T_1, F_{432}^1 and F_{134}^1 and for T_2, F_{413}^2 and F_{312}^2 are determined. The remaining two couples of faces might be chosen arbitrarily.

Observe that F_{432}^1 and F_{134}^1 are represented, in the glued configuration, by F_{342} and F_{543} respectively. Also, F_{413}^2 and F_{312}^2 are represented by F_{326} and F_{625}.

We have to verify compatibilities in the definition. Namely, that the side pairings maps the edges between them and that the tetrahedra defined by the faces above do not intersect else than in their common faces. We state the compatibility of the edges as a Lemma whose proof is a straightforward computation.

6.4. **Lemma.** *The finite edges between the flags are compatible with the side pairings.*

The second Lemma is the verification that the T_1 and T_2 are well defined, that is, as for T_0, their faces intersect only at common edges. Finally, we prove that the three tetrahedra intersect only at common faces. The proof is a sequence of tedious arguments as in the proof that T_0 was well defined but one can be convinced by carefully looking at Figure 13.

6.5. **Proposition.** *The gluing of the three tetrahedra T_0, T_1 and T_2 forms a polyhedron in the flag space.*
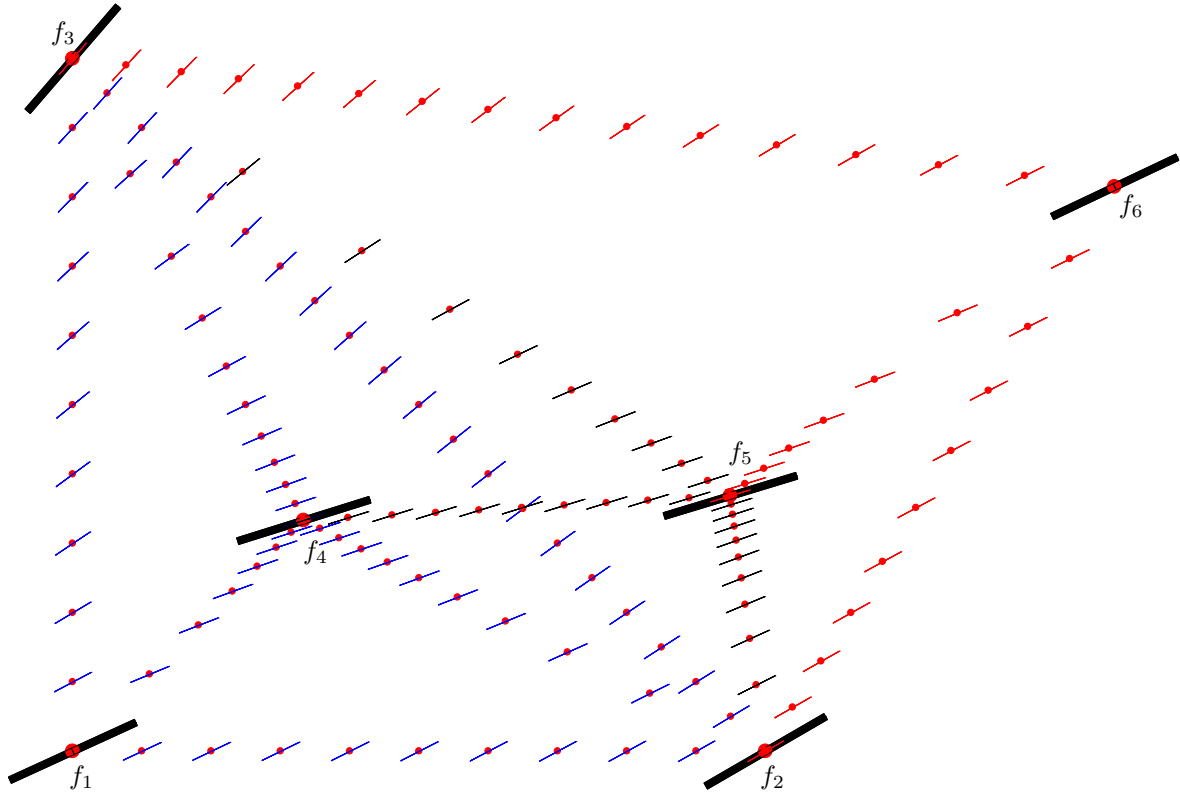
FIGURE 13. Gluing the 3 tetrahedra projected in the preferred chart

6.6. **The structure around the edges.** There are three edges in the quotient manifold. They are represented by the edges E_{23}, E_{24} and E_{34} in the first tetrahedron T_0. As far as the topological gluing is concerned, the number of tetrahedra around each edge are 8, 4 and 6 respectively (we show the schematic diagram of the gluing for each edge in figures 14 and 15). In order to prove that we have a genuine flag structure on the quotient manifold we should prove that the gluing of the tetrahedra around each of the three edges has no branching. That is, that the gluing around each edge gives a neighborhood of the edge.

We state the result in the following proposition. Its proof, again, is a tedious verification. Heuristically, one can understand the neighborhood of an edge by following the vertices of the tetrahedra that one adjoins to the edge. Turning around the edge corresponds to turning the angle of the projected line of the flag in the vertex in such a way that increasing the angle makes the tetrahedron go up and decreasing the angle makes the tetrahedron go down. In Figure 16 we show the 4 tetrahedra around the edge E_{24}. One can observe that the last point adjoined has the projected line of angle lower than the others. The tetrahedra adjoined will
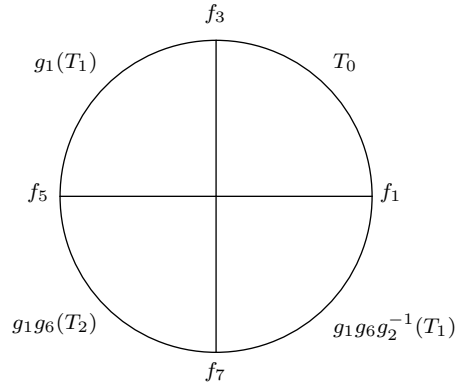
FIGURE 14. A schematic picture of a neighborhood around the edge $E_{23} = [f_2, f_4]$, where the segments stand for the faces with the common edge E_{23} denoted by the origin and the arcs and the regions between two segments stand for the neighborhoods contained in one tetrahedron.

be bellow the original two. In Figure 17 we show 5 of the 6 tetrahedra around the edge E_{34}. Here we have to add three more points to the original 3 tetrahedra. Observe that the first two have lines of decreasing angle but the last point increases the angle in order to complete the turn. In Figure 18 we show the vertices of the 8 tetrahedra around the edge E_{23}.

6.7. **Proposition.** *Along each of the three edges E_{13}, E_{24} and E_{34} the gluing of the tetrahedra defines a neighborhood.*

As a consequence of the propositions above we obtain our conclusion:

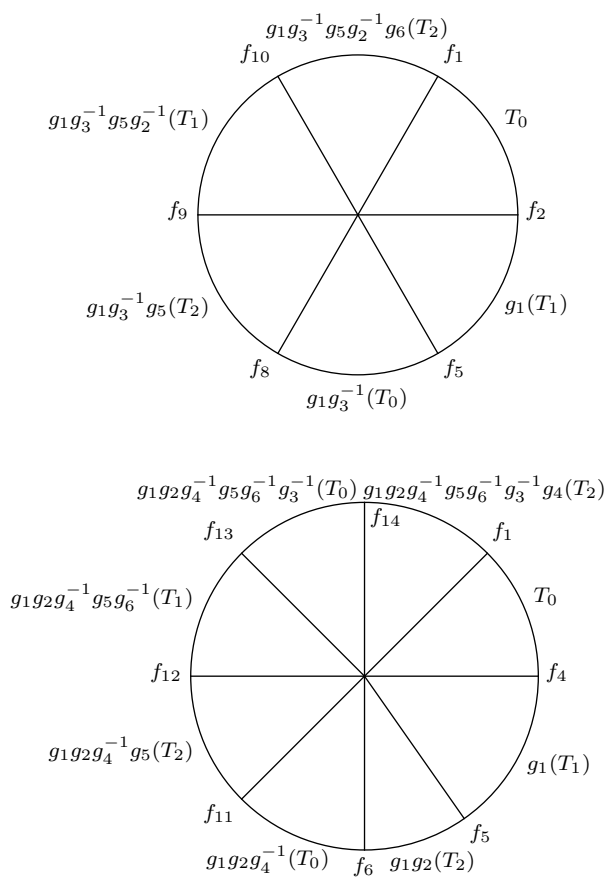6.8. **Theorem.** *The manifold $m009$ has a flag structure whose holonomy map is boundary unipotent.*
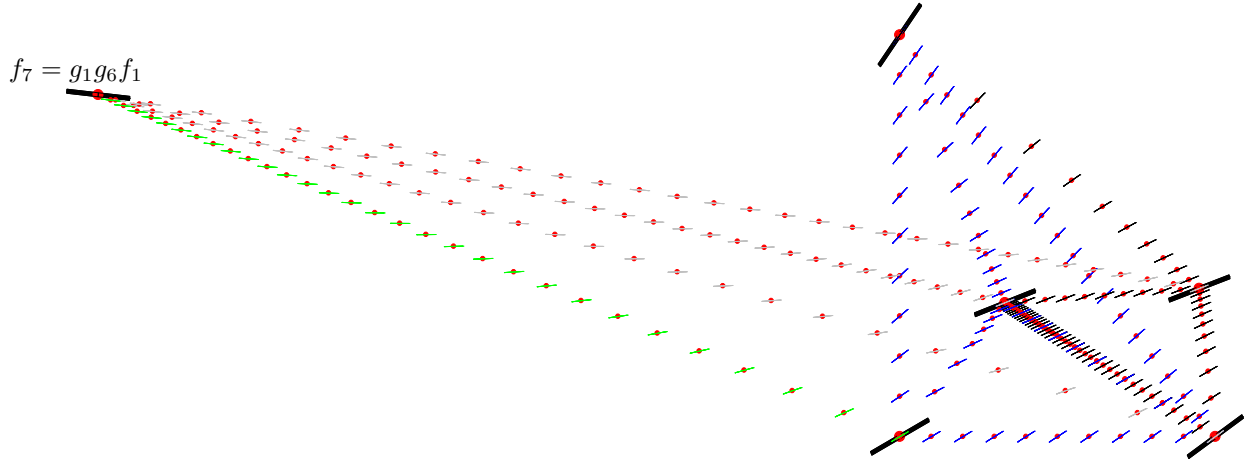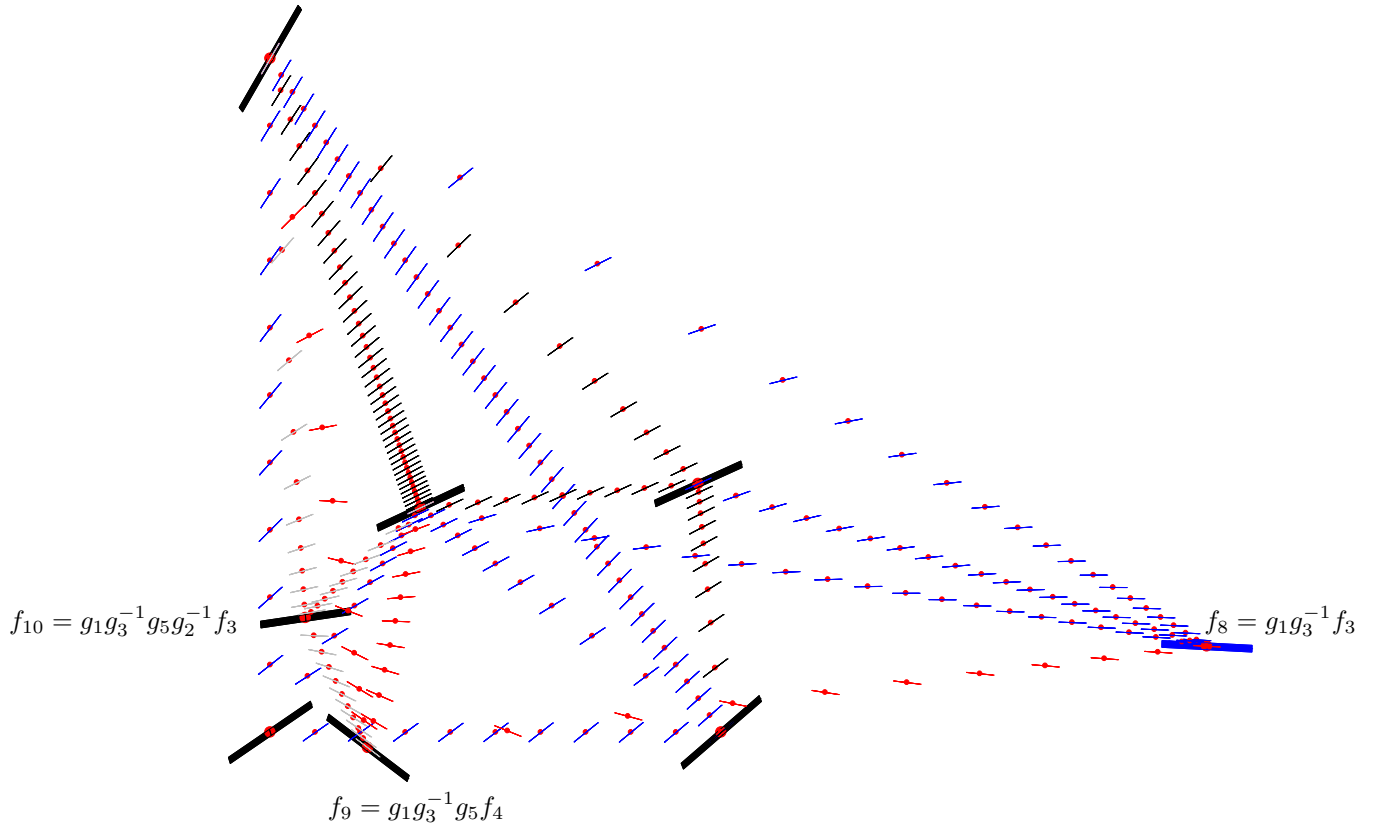
FIGURE 15. A schematic picture of a neighborhood around the edges $E_{23} = [f_2, f_3]$ and $E_{34} = [f_3, f_4]$.

FIGURE 16. Tetrahedra around the edge E_{24}.

FIGURE 17. Tetrahedra around the edge E_{34}.

$$f_{14} = g_1 g_2 g_4^{-1} g_5 g_6^{-1} g_3^{-1} f_3$$

$$f_{11} = g_1 g_2 g_4^{-1} f_2$$

$$f_{12} = g_1 g_2 g_4^{-1} g_5 f_4$$

$$f_{13} = g_1 g_2 g_4^{-1} g_5 g_6^{-1} f_4$$

FIGURE 18. Vertices of tetrahedra around the edge E_{23}. The group of 6 points in the center can be zoomed to coincide with Figure 13.

7. Appendix

In order to help the reader verify computations we list explicitly the side pairings we used. Note that we simplify notations denoting matrices by the same letters as the maps. First we let

$$
\begin{aligned}
u_1 &= 1 - \frac{1}{u_{12}} = \frac{2}{\gamma + 3}; \\
u_2 &= 1 - u_{21} = 1 - \gamma; \\
u_3 &= u_{34} = \frac{\gamma - 2}{\gamma}; \\
u_4 &= \frac{1}{1 - u_{43}} = \frac{1}{2 + \gamma}; \\
w_1 &= 1 - \frac{1}{w_{12}} = \frac{2}{2 - \gamma}; \\
w_2 &= 1 - w_{21} = 2 + \gamma; \\
w_3 &= w_{34} = \frac{\gamma + 3}{\gamma + 1}; \\
w_4 &= \frac{1}{1 - w_{43}} = \frac{1}{1 - \gamma}; \\
v_1 &= 1 - \frac{1}{v_{12}} = -2 - \gamma; \\
v_2 &= 1 - v_{21} = \frac{\gamma - 1}{\gamma - 2}; \\
v_3 &= v_{34} = \frac{1}{\gamma + 3}; \\
v_4 &= \frac{1}{1 - v_{43}} = \frac{\gamma - 2}{\gamma - 1};
\end{aligned}
$$

The the side pairings are given by
$F_{234}^0 = g_1(F_{243}^1)$

$$
g_1 = \begin{bmatrix} -\lambda_3 & 0 & \lambda_3 \\ -\lambda_1 - \lambda_3 & \lambda_1 & \lambda_3 \\ -\lambda_3 + \lambda_2 & 0 & \lambda_3 \end{bmatrix}.
$$

$$
\lambda_2 = \lambda_1(v_3 - 1)(1 - u_4); \qquad \lambda_3 = \lambda_1/((v_4 - 1)(1 - u_3)).
$$

$F_{142}^1 = g_2(F_{241}^2)$

$$
g_2 = \begin{bmatrix} 0 & \delta_3 & \delta_2 - \delta_3 \\ \delta_1 & 0 & \delta_2 - \delta_1 \\ 0 & 0 & \delta_2 \end{bmatrix}.
$$

$$
\delta_2 = \delta_1 v_1(w_2 - 1)/(w_2(v_1 - 1)); \qquad \delta_3 = \delta_1(1 - v_4)(1 - w_4)/(v_4 w_4).
$$

$F_{142}^0 = g_3(F_{314}^1)$

$$
g_3 = \begin{bmatrix} \alpha_2 & -\alpha_2 - \alpha_1 & \alpha_1 \\ \alpha_2 & \alpha_3 - \alpha_2 & 0 \\ \alpha_2 & -\alpha_2 & 0 \end{bmatrix}.
$$

$$
\alpha_2 = \alpha_1 u_2 v_4/(1 - u_2); \qquad \alpha_3 = \alpha_1 u_4(v_1 - 1)/(u_4 - 1).
$$

$$F^0_{134} = g_4(F^2_{143})$$

$$g_4 = \begin{bmatrix} \beta_1 & -\beta_1 - \beta_3 & \beta_3 \\ 0 & -\beta_3 & \beta_3 \\ 0 & \beta_2 - \beta_3 & \beta_3 \end{bmatrix}.$$

$$\beta_2 = \beta_1 u_4(1 - w_3)/w_3; \qquad \beta_3 = \beta_1 u_3/(w_4(1 - u_3)).$$

$$F^0_{123} = g_5(F^2_{213})$$

$$g_5 = \begin{bmatrix} 0 & \epsilon_1 & 0 \\ \epsilon_2 & 0 & 0 \\ 0 & 0 & \epsilon_3 \end{bmatrix}.$$

$$\epsilon_2 = \epsilon_1 u_3 w_3; \qquad \epsilon_3 = \epsilon_1 u_2/w_1$$

$$F^1_{123} = g_6(F^2_{342})$$

$$g_6 = \begin{bmatrix} -\zeta_1 & 0 & \zeta_1 \\ \zeta_2 & 0 & 0 \\ -\zeta_3 & \zeta_3 & 0 \end{bmatrix}.$$

$$\zeta_2 = \zeta_1 v_3(w_2 - 1); \qquad \zeta_3 = \zeta_1 v_2(1 - w_4).$$

Thinking the side pairings as hyperbolic transformations we can obtain a presentation of the fundamental group of $m009$. Indeed, the side pairings of the (hyperbolic) polyhedron formed by gluing the tetrahedra (as in Figure 13) according to $g_1 : (243)^1 \to (234)^0$ and $g_2 : (142)^2 \to (241)^1$ are

$$s_3 = g_3 g_1^{-1}, \quad s_4 = g_4 g_2^{-1} g_1^{-1} \quad s_5 = g_5 g_2^{-1} g_1^{-1} \quad s_6 = g_1 g_6 g_2^{-1} g_1^{-1}.$$

The three edge cycles give the following relations

$$s_6 s_3^{-1}, \quad s_4^{-1} s_5 s_6^{-1} s_3^{-1} s_4 s_5^{-1}, \quad s_3^{-1} s_5 s_6 s_4^{-1}$$

and the presentation of the fundamental group $\Gamma = \pi_1(m009)$ of the manifold m009 can be simplified to be

$$\Gamma = \langle \ s_3, s_5 \ | \ [s_3^{-1}, s_5^{-1}] s_3^{-2} [s_3^{-1}, s_5] \ \rangle.$$

The manifold $m009$ is fibered over the circle. From the presentation we obtain that its fundamental group Γ has abelianization

$$\Gamma/[\Gamma, \Gamma] = \frac{\mathbb{Z}}{2\mathbb{Z}} \oplus \mathbb{Z}.$$

Indeed, from the presentation we observe that $s_3^2 \in [\Gamma, \Gamma]$. We conclude that the image of s_5 in $\Gamma/[\Gamma, \Gamma]$ is non-trivial and generates an infinite cyclic group.

One can also check (using SnapPea for instance and comparing fundamental groups) that $m009$ is the same as the manifold b$_{++}$RRL which is the punctured torus bundle defined by the pseudo-Anosov

$$\begin{bmatrix} 3 & 2 \\ 1 & 1 \end{bmatrix}.$$

However, a computation with the matrices of s_3 and s_5 (we warn the reader that we also write s_i for the image of s_i under the holonomy representation, by abuse of notation) shows that the holonomy group is contained in a triangle group of type $(3, 3, 5)$. Indeed, s_3 is of order 5, $s_3 s_5$ and $s_3^2 s_5$ are of order 3. On the other hand s_5 is unipotent.

References

[1] T. Barbot, Flag structures on Seifert manifolds, Geometry and Topology 5 (2001) 227-266.

[2] N. Bergeron, E. Falbel, A. Guilloux, Tetrahedra of Flags, Volume and Homology of SL(3). Preprint 2011.

[3] D. Cooper, D. Long, S. Tillmann, On Convex Projective Manifolds and Cusps (2011). arXiv:1109.0585v2.

[4] M. Deraux, In preparation.

[5] E. Falbel, A spherical CR structure on the complement of the figure eight knot with discrete holonomy, J. Diff. G. 79 (2008), 69-110.

[6] E. Falbel, P.-V. Koseleff, F. Rouillier, Representations of fundamental groups of 3-manifolds into PGL$(3, \mathbb{C})$: exact computations in low complexity. Preprint 2013.

[7] I. M. Gelfand, R. D. MacPherson, Geometry in Grassmannians and a Generalization of the Dilogarithm. Advances in Mathematics 44 (1982), 279-312.

[8] W. Thurston, The geometry and topology of 3-manifolds, Princeton lecture notes (1978-1981).

INSTITUT DE MATHÉMATIQUES DE JUSSIEU, UNIVERSITÉ PIERRE ET MARIE CURIE, 4, PLACE JUSSIEU, F-75252 PARIS, FRANCE

INRIA, OURAGAN, PARIS-ROCQUENCOURT

DEPARTAMENTO DE CIÊNCIAS EXATAS E APLICADAS, INSTITUTO DE CIÊNCIAS EXATAS E APLICADAS, UNIVERSIDADE FEDERAL DE OURO PRETO, RUA 36, N. 115, BAIRRO LOANDA, 35.931-008 JOAO MONLEVADE - MG - BRAZIL